doi: 10.4149/gpb_2024046

Synthesis of *Epimedium* extract selenium nanoparticles and evaluation their efficacy against lung cancer

Guangying Fu[1] and Jin Tong[2]

[1] *Department of Respiratory Medicine, The Second Affiliated Hospital of Chongqing Medical University, Chongqing, China*
[2] *Department of Critical Care Medicine, The Second Affiliated Hospital of Chongqing Medical University, Chongqing, China*

Abstract. Lung cancer, the foremost cause of cancer-related mortality worldwide, necessitates the exploration for novel anti-lung cancer therapeutics to enhance efficacy and reduce adverse effects. Targeting selenium in the tumor microenvironment has become a new strategy for the treatment of lung cancer. The objective of this study was to synthesize novel selenium nanoparticles (EBM-SeNPs) using aqueous extracts derived from *Epimedium brevicornum Maxim* and investigate its structural characteristics and inhibitory effects against lung cancer. The physicochemical properties of EBM-SeNPs were characterized from multiple aspects using a variety of methods. The CCK-8, flow cytometry, wound healing assay, Western blot and the cell derived xenograft model were conducted to evaluate the antitumor efficacy *in vivo* and *in vitro*. EBM-SeNPs were approximately spherical and exhibited superior dispersivity and stability in water solution. And EBM-SeNPs did not display any specific cytotoxicity against human liver cells. However, they showed outstanding capability to induce apoptosis in lung cancer cells, thereby effectively suppressing their growth and migratory potential. Furthermore, EBM-SeNPs demonstrated a reduction of tumor and an increase in immune organ index of tumor-bearing mice. Collectively, the EBM-SeNPs may be an effective and safe option for the treatment of lung cancer.

Key words: Selenium — Nanoparticles — *Epimedium* — Anti-lung cancer — Aqueous extracts — Efficacy and safety

Abbreviations: DDP, cisplatin; DLS, dynamic light scattering; EBM, *Epimedium brevicornum Maxim* extract, EBM-SeNPs, EBM-loaded selenium nanoparticles; ECL, enhanced chemiluminescence; EDX, energy dispersive X-Ray spectroscopy; EGFR-TKIs, epidermal growth factor receptor-tyrosine kinase inhibitors; FBS, fetal bovine serum; HCC, hepatocellular carcinoma; HR-LCMS, high-resolution liquid chromatography-mass spectroscopy; HRP, horseradish peroxidase; ICP-OES, coupled plasma optical emission spectrometer; NS, normal saline; PDI, polymer dispersity index; PI, propidium iodide; STR, short tandem repeat; TCM, Chinese traditional medicine; TEM, transmission electron microscopy.

Highlights

- EBM-SeNPs were prepared using an environmentally sustainable approach and the physicochemical properties were characterized.
- The efficacy against lung cancer and biocompatibility of EBM-SeNPs were assessed both *in vitro* and *in vivo*.
- Our findings have revealed a novel biocompatible nanocomposite for the treatment of lung cancer.

Correspondence to: Jin Tong, Department of Critical Care Medicine, The Second Affiliated Hospital of Chongqing Medical University, No. 76, Linjiang Road, Chongqing 400010, China
E-mail: 300291@hospital.cqmu.edu.cn; tongjin01234@163.com

Introduction

The high incidence of lung cancer is a major contributor to cancer-related mortalities on a global scale (Schabath and Cote 2019; Bade and Dela Cruz 2020; Oliver 2022). Due to the high degree of malignancy and rapid tumor progression, patients with lung cancer are often diagnosed with advanced lung cancer and have poor prognosis (Lahiri et al. 2023). For advanced lung cancer, epidermal growth factor receptor-tyrosine kinase inhibitors (EGFR-TKIs) and immunotherapy are commonly used in clinical practice. However, considering the frequent mutation of drugs targeting specific gene after long-term application and the low responsiveness of immunotherapy, new safe and effective treatment strategies need to be developed urgently (Li et al. 2021, 2024; Luo Z et al. 2024).

In recent years, the study of tumor microenvironment has provided the potential to develop new therapeutic strategies, and the balance of nutrients in the tumor microenvironment has been increasingly studied (Fu et al. 2022). Selenium (Se), as an essential trace element in humans and animals, has been reported to demonstrate immunomodulatory and antitumor properties (Zhang et al. 2018; Zhou et al. 2021; Dogaru et al. 2023; Maia et al. 2023). Clinical studies have demonstrated that selenium can reduce the incidence of lung cancer and improve the sensitivity of lung cancer cells to radiotherapy, meaning that selenium compounds may serve as anticancer agents (Nasir et al. 2020; Manjunatha et al. 2021; Martínez-Esquivias et al. 2022; Zhang et al. 2023a). Stable and biocompatible selenium nanoparticles (SeNPs) have the potential to inhibit the potential toxicity of selenium and improve the targeting of drugs (Yan et al. 2018; Zhang et al. 2019; Chen et al. 2022; Sampath et al. 2024). Considering the anti-tumor effects of SeNPs and their role as drug carriers, the use of SeNPs to deliver anti-tumor drugs to the tumor site resulting in a stronger tumor-targeting effect is a current research hotspot.

The *Epimedium brevicornum Maxim* perennial herbaceous plant holds significant importance in the context of Chinese traditional medicine (TCM) (Rong et al. 2015; Zhang et al. 2022) and has promising therapeutic effects on osteoporosis, chronic nephritis, reproductive system diseases, cancer, and reduced immune function (Zhao et al. 2019; Liu et al. 2020; Ke et al. 2023; Tong et al. 2023; Luo P et al. 2024). Nevertheless, when administered alone, it suffered from several limitations such as the nonspecific scope of action, high dosage, and low bioavailability. Notably, Icaritin, the active ingredient from *Epimedium brevicornum Maxim*, has been demonstrated promising therapeutic effects in hepatocellular carcinoma (HCC) patients (Lu et al. 2022). Recent studies have reported that the active components of *Epimedium brevicornum Maxim* have potent anti-tumor effects on lung cancer cells (Song et al. 2012; Lu et al. 2019). As a drug carrier that can improve drug targeting and bioavailability, SeNPs is often combined with plant extracts to form new nanomedicine to improve the efficacy of plant extracts against diseases (Veeraraghavan et al. 2021; Menon et al. 2022; Almukainzi et al. 2023). However, there have been limited studies reporting on the use of *Epimedium brevicornum Maxim* extract (EBM) as a stabilizer for SeNPs synthesis against lung cancer. Therefore, the synthesis of EBM and SeNPs is a very promising anti-tumor strategy.

The present study included the utilization of *Epimedium brevicornum Maxim* water extract in the synthesis of EBM-SeNPs, followed by an analysis of the physicochemical properties of EBM-SeNPs. The antitumor and cytotoxic properties of EBM-SeNPs were investigated *in vitro*. Similarly, the *in vivo* biocompatibility of EBM-SeNPs was also evaluated, and it has been confirmed that EBM-SeNPs has superior anticancer and immunological effects *in vivo* when compared to both EBM and bare selenium nanoparticles (B-SeNPs). This study provided a new anticancer strategy for the treatment of lung cancer.

Materials and Methods

Materials

EBM was purchased from a local Chinese pharmacy and produced in Qinling Mountains, Shanxi Province, China. Selenious acid sodium (Na_2SeO_3) was acquired from Alfa Aesar Chemical Co. Ltd. (Shanghai, China). The Shanghai Beyotime Biotechnology Co. Ltd. (Shanghai, China) provided cisplatin (DDP). All the antibodies were acquired from Chengdu Zen-Bioscience Co. Ltd.

Preparation of EBM

The EBM extract was prepared by mixing *Epimedium brevicornum Maxim* crude powder with deionized water in a ratio of 1:10 (g/ml), followed by decoction at 85°C for 3 hours. The resulting mixture was then filtered and concentrated to obtain the EBM extract which was then lyophilized to obtain a powder for further experiment.

Synthesis of EBM-SeNPs

Based on previous experience (Vundela et al. 2021) and a slight modification, the reaction steps in brief were as follows: EBM and Na_2SeO_3 solution were thoroughly mixed using a magnetic stirrer followed by the dropwise addition of freshly prepared $C_6H_8O_6$ solution. As reported previously, it has been observed that a molar ratio of 1:4 between selenious acid sodium (Na_2SeO_3) and ascorbic acid ($C_6H_8O_6$) is advantageous for the complete reduction

of sodium selenite, leading to the formation of more stable SeNPs (Wang et al. 2019; Hernández-Díaz et al. 2021). Based on these considerations, we set total amount of Na_2SeO_3 and $C_6H_8O_6$ to 0.2 and 0.8 mM, respectively, and introduced them into a reaction system with a volume of 10 ml. Then we continuously adjusted the EBM concentration (2, 4, 6, 8, 10, 12, 14 mg/ml), the reaction temperature (0, 25, 50, 75, 100°C) and the reaction time (0.5, 1.0, 1.5, 2.0, 2.5, 3.0 hours). We employed the control variable method, sequentially determining individual parameters while optimizing the remaining conditions for EBM-SeNPs synthesis. After the completion of the reaction, the solution was dialyzed in ultrapure water for 72 h to remove excess reaction precursors. Synthesis of B-SeNPs was carried out in the same way, except for an equal volume of ultrapure water used in place of EBM.

The optimal reaction conditions were ascertained for the synthesis of stable EBM-SeNPs: 8 mg/ml of EBM, 0.2 mM Na_2SeO_3 and 0.8 mM $C_6H_8O_6$, 10 ml reaction system, 37°C temperature and 2 h time duration.

Characterization of EBM-SeNPs

Initial confirmation of EBM-SeNP synthesis was obtained using a UV spectroscopic investigation ranging from 200 to 800 nm. The morphology of EBM-SeNPs was studied with transmission electron microscopy (TEM) while the hydrodynamic diameter and zeta potential were measured by a Zetasizer Nano ZS90 particle analyzer. The possible functional groups in EBM-SeNPs were assessed using FT-IR spectra and the determination of elemental composition of the EBM-SeNPs was carried out by energy dispersive X-Ray spectroscopy (EDX) analysis. The content of the Se element in EBM-SeNPs was quantified using inductively coupled plasma optical emission spectrometer (ICP-OES).

Cell culture

The human NSCLC cell line A549 was purchased from Boster Biological Technology Co., Ltd (Wuhan, China), the LLC cell line (mouse lung cancer cell line) was purchased from SUNNCELL Co., Ltd (Wuhan, China), and the L-02 cell line (human normal heptical cell line) was offered from the American Type Culture Collection (ATCC; Manassas, VA, USA). All cells were identified by short tandem repeat (STR) before leaving the factory. All the obtained cell lines were cultured in DMEM medium supplemented with 10% fetal bovine serum (FBS, Biological Industries, Kibbutz Beit Haemek, Israel) and 1% penicillin-streptomycin at 37°C in an atmosphere of 5% CO_2. All cells were tested for mycoplasma every 2 months using Mycoplasma PCR Detection Kit (Beyotime, China).

Cell viability assay

The effects of EBM-SeNPs on the viability of A549 and L-02 cells were investigated by CCK-8 assay (Apexbio Biotechnology Science and Technology Co. Ltd., Suzhou, China). Briefly, A549 and L-02 cells were seeded in a 96-well plate at a density of 5×10^3 cells/well for 24 h and then treated with various concentrations of B-SeNPs, EBM, EBM-SeNPs (0, 10, 20, 40, 80, 160 μg/ml). After 24 h of incubation, the CCK-8 reagent was incorporated and subjected to further incubation for 1 h. A microplate reader was employed to measure absorbance at 450 nm. DDP (5 ug/ml) was used as a positive control. The following formulae were used for calculations (Zhu et al. 2022): Inhibition ratio (%) = $[OD_{control} - OD_{treatment}]/ [OD_{control} - OD_{blank}] \times 100\%$; Cell viability (%) = $[OD_{treatment} - OD_{blank}]/ [OD_{control} - OD_{blank}] \times 100\%$.

Cell cycle analysis and cell apoptosis

Flow cytometry was utilized to identify the inhibitory effect of EBM-SeNPs on the cell cycle of A549 cells. Briefly, A549 cells were incubated in 6-well plates for 24 h after being treated with B-SeNPs, EBM, or EBM-SeNPs. Cells cultured in drug-free medium were used as the control group. Then the cells received a one-time wash using pre-chilled PBS. Propidium iodide (PI) (Shanghai Beyotime Biotechnology Co. Ltd., Shanghai, China) staining was performed after cell fixation with 70% ethanol for a duration of 8 h at 4°C. The samples were then analyzed by flow cytometry. Similarly, cells were suspended and stained with annexin V-FITC and PI (Shanghai Beyotime Biotechnology Co. Ltd., Shanghai, China) after being washed and centrifuged. The apoptosis of the cells was then evaluated *via* flow cytometry.

Wound healing assay

The A549 cells were cultured to 100% confluency in a six-well plate and the incision was performed by using a 100 μl pipette. After washing with PBS for 3 times, the cells were cultured in a medium supplemented with 2% serum containing different drugs (B-SeNPs, EBM, or EBM-SeNPs). Then the cells were imaged using a microscope from Olympus Corporation in Tokyo, Japan, after 0, 24 and 48 h of incubation.

Western blotting assay

The cell protein was extracted from each group, and the protein concentration was quantified using the BCA assay (Shanghai Beyotime Biotechnology Co. Ltd., Shanghai, China). The protein was then transferred onto a PVDF

(0.22 μm) membrane after being resolved by 10% SDS-PAGE. Membranes were incubated with primary antibodies overnight at 4°C following blocking with 5% skim milk. Following that, the samples were subjected to blotting using secondary antibodies conjugated with horseradish peroxidase (HRP) and analyzed with an enhanced chemiluminescence (ECL) detection system (Bio-Rad, USA).

Animal experiments

The female C57BL/6 mice (6–7 weeks) were obtained from the Laboratory Animal Center of Chongqing Medical University and housed under specific pathogen-free conditions in the Laboratory Animal Center of the Second Affiliated Hospital of Chongqing Medical University. All experimental animal procedures were approved by the Animal Ethics Committee of the Second Affiliated Hospital of Chongqing Medical University (IRB No. IACUC-SAHCQMU-2023-0021). After a one-week acclimatization period, 5×10^6 LCC cells were injected into the right armpit of the mice. The tumor volume was calculated using the following formula (Jiang et al. 2024): Tumor volume = $(a\times b^2)/2$, where a is the maximum diameter of the tumor and b is the minimum diameter of the tumor. When the tumor volume reached 50–100 mm^3, mice were randomly allocated into five groups, each comprising six mice. Then, normal saline (NS, 200 μl/day), B-SeNPs (2 mg/kg/day), EBM (2 mg/kg/day), EBM-SeNPs (2 mg/kg/day), and DDP (4 mg/kg/3 days) were respectively administered to the mice by intraperitoneal injection for 21 days. The weights and the tumor volume of mice were recorded on alternate days.

After that, the tumors and immune organs were harvested and weighed to evaluate tumor inhibition rate and organ index separately. The peripheral blood samples were collected for the examination of kidney and liver function. The tumors and major organs (heart, liver, spleen, lung, and kidney) were preserved in 4% polyoxymethylene for H&E and PCNA staining. The tumor inhibition rate and organ indexes were calculated as follows: organ indexes = spleen (thymus) weight/body weight × 100%; tumor inhibition rate (%) = (1 – a/b) × 100%, where a is the weight of the tumors of the treatment groups, and b is the average weight of the tumors of the control group.

Statistical analysis

Statistical analysis was performed on all the data related to multiple groups using one-way ANOVA with SPSS software (version 16.0, SPSS, Inc., Chicago, IL). The findings were presented as the mean ± SD, and differences were defined as significant at a p value < 0.05.

Results

Synthesis and characterization of EBM-SeNPs

The change in color of the reaction solution can typically serve as an initial indicator for assessing the synthesis of SeNPs. The coloration of SeNPs, as observed in previous studies (Mikhailova 2023; Adam-Dima et al. 2024; Haji Mehdi Nouri et al. 2024), primarily exhibits shades ranging from orange to brick red, which can be attributed to variations in the concentration of SeNPs and types of precursors. The transformation of the colorless Na_2SeO_3 solution to a brick-red color served as preliminary confirmation of the synthesis of EBM-SeNPs in present investigation (Gunti et al. 2019). As illustrated in Figure 1A, the UV-vis spectrum revealed a maximal characteristic peak at 265 nm which further indicated the formation of EBM-SeNPs (Hernández-Díaz et al. 2021). And the UV-vis spectrum of EBM-SeNPs demonstrated discernible attributes in comparison to its synthetic precursors, thereby signifying the chemical and physical interaction between the components (Cao et al. 2021). Additionally, the absorption maximal peak exhibited temporal consistency for two weeks, indicating the stability of EBM-SeNPs (Fig. 1B). Finally, the optimal reaction conditions were ascertained for the synthesis of stable EBM-SeNPs: 8 mg/ml of EBM, 0.2 mM Na_2SeO_3 and 0.8 mM $C_6H_8O_6$ at 37°C for 2 h in a 10 ml reaction system.

TEM was utilized to examine the morphology of EBM-SeNPs. Unlike B-SeNPs, which exhibited significant aggregation, most of EBM-SeNPs appeared as dispersed, nearly spherical particles with an average size of 40 nm, and were significantly smaller than B-SeNPs (Fig. 1C). Consisting with previous investigations (Yang et al. 2023), the presence of EBM on the surface of SeNPs is believed to alter the size of SeNPs while serving as a nano-stabilizer. The sizes of EBM-SeNPs observed under TEM were smaller than that under the dynamic light scattering (DLS), which was calculated to be 65.03 ± 1.96 nm (Fig. 1D). The variations in measurements could be attributed to the fact that DLS assessed the diameter in the water-swelling state, whereas TEM measured the diameter in the dry state. The polymer dispersity index (PDI) of EBM-SeNPs was reported to be 0.383, which indicated a good distribution of these particles. The zeta potential of EBM-SeNPs was determined to be −22.95 ± 0.76 mV (Fig. 1E), indicating the presence of substantial negative charges on the surface of nanoparticles. These charges could create repulsion forces, contributing to the increased stability of the nanoparticles in the solution.

FT-IR analysis was performed to determine the presence of EBM on the surface of SeNPs and to examine the interaction between EBM and SeNPs in EBM-SeNPs (Fig. 1F). The strong absorption peaks at 3396 and 2926 cm^{-1} in the FT-IR spectrum of EBM were attributed to stretching

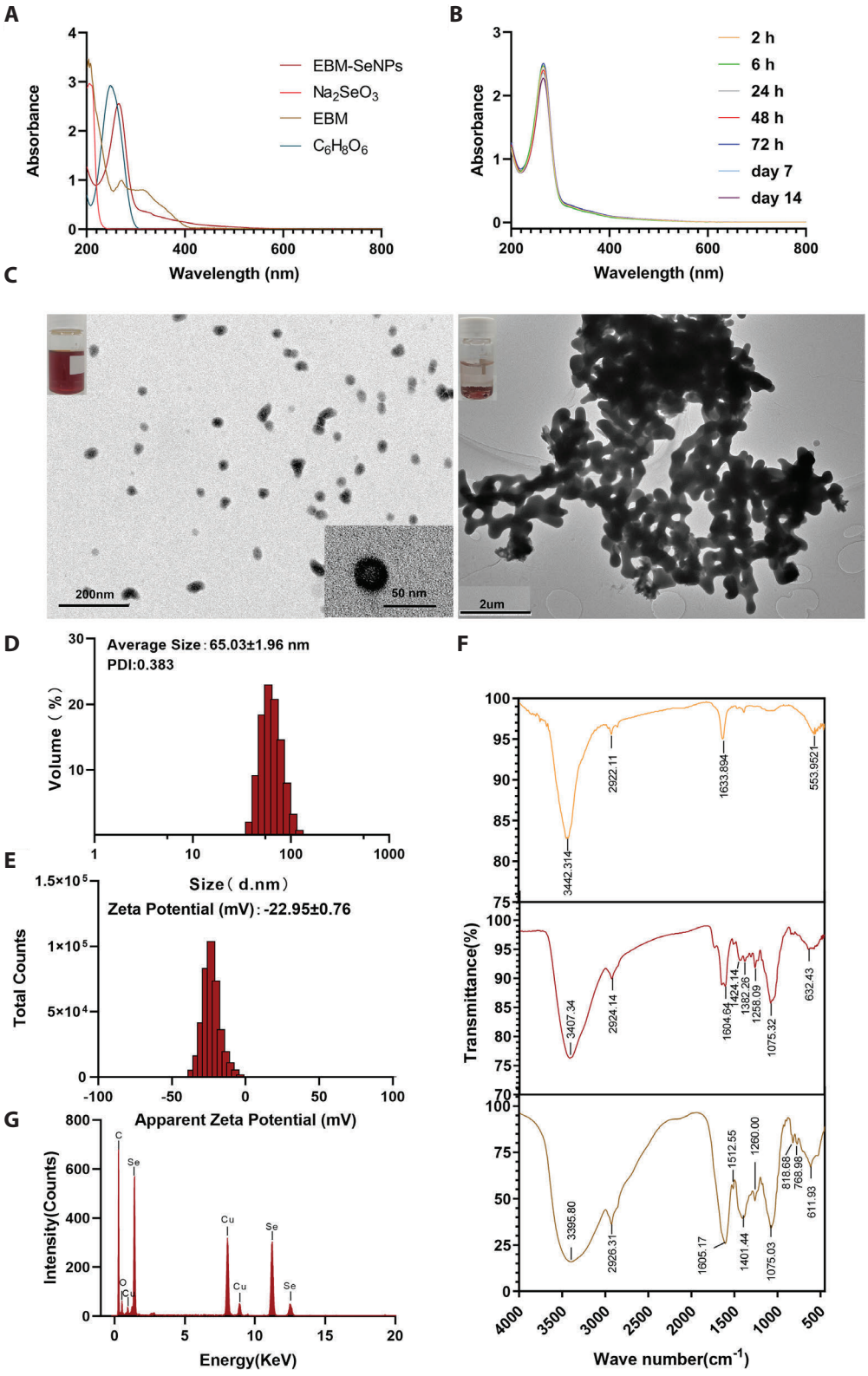

Figure 1. The UV-vis absorption spectra and characterization of EBM-SeNPs. **A.** The UV-vis spectra of EBM-SeNPs, EBM, Na_2SeO_3, and $C_6H_8O_6$. **B.** The UV-vis spectra of EBM-SeNPs at different time. **C.** TEM images of EBM-SeNPs and B-SeNPs. **D, E.** DLS analysis of EBM-SeNPs. **F.** FTIR analysis of B-SeNPs, EBM-SeNPs and EBM. **G.** EDX analysis of EBM-SeNPs. (See online version for color figure.)

vibrations of the O-H and C-H groups, respectively (Hassan et al. 2021). The peak at 1605 and 1075 cm^{-1} can be respectively attributed to the C–O and C–O–C stretching (Wang et al. 2021; Vu et al. 2023). The peaks observed in the FT-IR spectrum of EBM-SeNPs were found to be identical, suggesting the existence of EBM in EBM-SeNPs. Specifically, a shift in the –OH peak from 3396 cm^{-1} (EBM) to 3407 cm^{-1} (EBM-SeNPs) was observed, indicating interactions between SeNPs and EBM through physical adsorption (Huong et al. 2023).

The elemental composition of EBM-SeNPs was thoroughly examined through EDX analysis. The confirmation of the effective synthesis of EBM-SeNPs was further supported by the presence of Se in the EDX spectroscopy data, as illustrated in Figure 2E. Meanwhile, the existence of Cu atoms can be attributed to the copper grids that served as the filament's support. According to ICP-OES, the mass percentage of Se in EBM-SeNPs was 43.5%.

To explore which substances in EBM might play a major role, HR-LCMS was carried out, and the Icariin, Epimedin A,

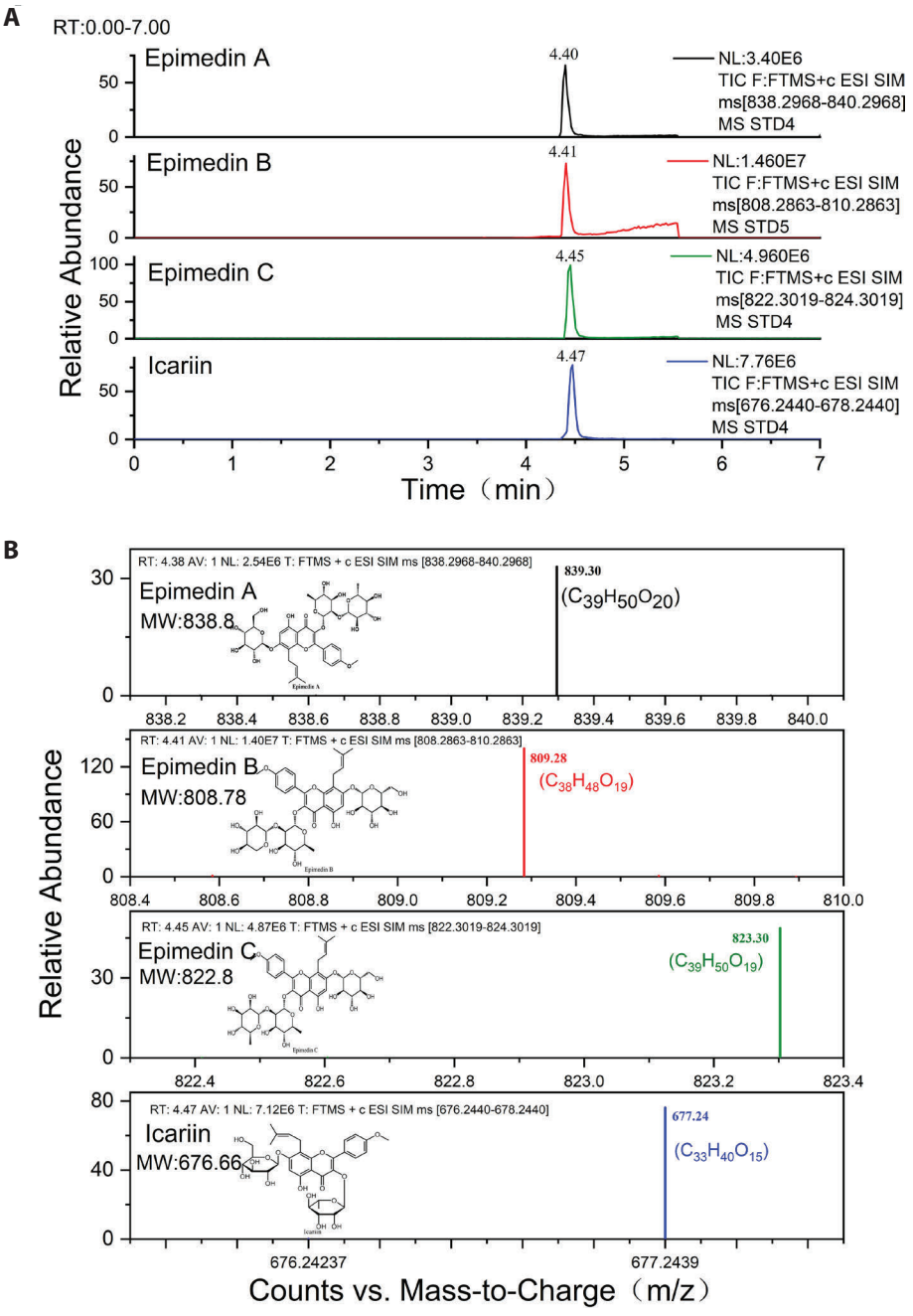

Figure 2. HR-LC/MS chromatogram of main active components in EBM. Liquid chromatograms (**A**) and Ion mass spectrometry (**B**) of Epimedin A, Epimedin B, Epimedin C and Icariin.

Epimedin B and Epimedin C were chosen to be detected in EBM as these compounds were clarified to be main active substance in EBM (Sha et al. 1997; Naseer et al. 2015). High-resolution liquid chromatography–mass spectroscopy (HR-LCMS) are reported in Figure 2. HR-LCMS study of the aqueous extracts from EBM revealed the presence of Epimedin A (Rt 4.40 min, MS 839.2946 m/z), Epimedin B (Rt 4.41 min, MS 809.2836 m/z), Epimedin C (Rt 4.45 min, MS 823.3021 m/z), and Icariin (Rt 4.47 min, MS 677.2440 m/z). These flavonoids were previously described as major anticancer compounds in EBM (Chen et al. 2024; Gu et al. 2017; Liu FY et al. 2023, Liu YM et al. 2023; Zhang et al. 2023b).

Antitumor effect of EBM-SeNPs in vitro

Cytotoxicity of EBM-SeNPs

The cytotoxicity of EBM-SeNPs on A549 and L-02 cells was evaluated using the CCK-8 assay. In Figure 3A, the inhibitory effects of both EBM-SeNPs and EBM on A549 cells were observed in a dose-dependent manner and EBM-SeNPs exhibited a stronger cytotoxic effect on lung cancer cells compared to EBM. B-SeNPs had minimal impact on the cells, which may be because B-SeNPs aggregated and produced precipitates incapable of interacting with cells (Yang et al. 2023). It is worth noting that the inhibition rate of EBM-SeNPs on A549 cells at a concentration of 40 ug/ml can reach up to 33%, which was comparable to the conventional chemotherapeutic drug DDP. The results suggested that EBM plays a pivotal role in determining the bioactivity of SeNPs, and the remarkable antitumor efficacy observed with EBM-SeNPs can be attributed to the synergistic interaction between EBM and SeNPs.

Studies have demonstrated that Se primarily accumulates in the liver and excessive Se intake can lead to liver damage (Urbankova et al. 2021; Singh et al. 2024). Therefore, to investigate the biocompatibility of these three drugs, human normal liver cell line L-02 was used as model cells. The results demonstrated that DDP significantly decreased the viability of L-02 cells. Interestingly, neither EBM, EBM-SeNPs, nor B-SeNPs exhibited any notable cytotoxic effects on L-02 cells even at a drug concentration of 160 ug/ml (Fig. 3B). Meanwhile, the cell survival rate of L-02 cells exhibited a gradual increase after treatment with lower doses of EBM-SeNPs, especially at 20 μg/ml and 40 μg/ml, which may be due to the provision of growth nutrients or the protective effects of low doses of EBM-SeNPs on liver cells. These results suggested that EBM-SeNPs showed excellent antitumor effects and good biocompatibility on normal cells. Considering the anti-tumor efficacy and hepatocyte safeguarding properties of EBM-SeNPs, subsequent investigations were conducted at a concentration of 40 μg/ml.

Pro-apoptotic effect of EBM-SeNPs on A549 cells

Previous studies have demonstrated that the promotion of apoptosis is regarded as one of the most pivotal mechanisms underlying the anti-tumor effects exerted by selenium-containing compounds (Shi et al. 2021). Flow cytometry was used to evaluate the apoptosis rate of A549 cells after being exposed to EBM-SeNPs. As shown in Figure 4A, both EBM-SeNPs and EBM significantly induced apoptosis in A549 cells compared to the control group. And compared to EBM, EBM-SeNPs significantly augmented the overall apoptotic rate of A549 cells, with a more pronounced occurrence of early apoptosis. These findings suggested that the

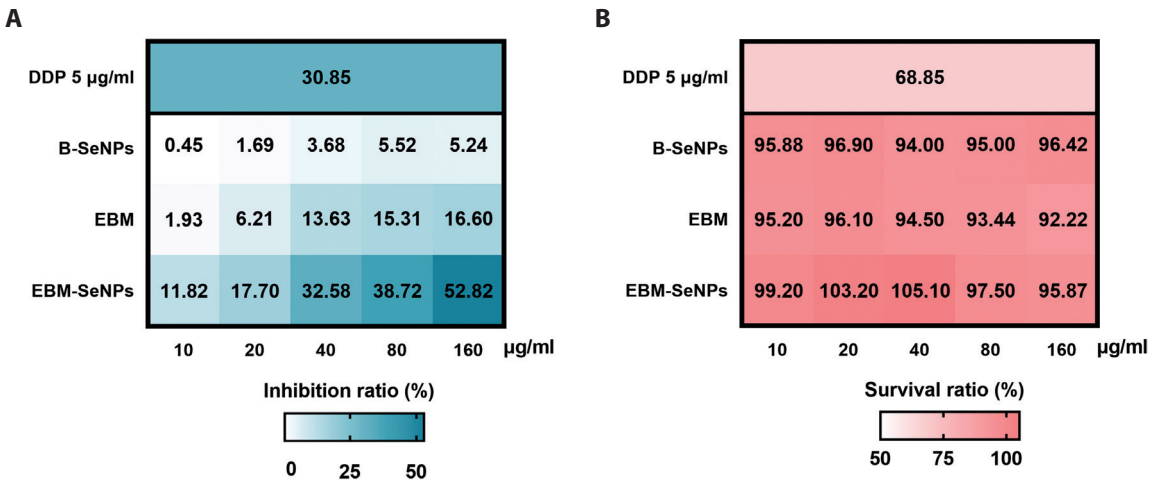

Figure 3. Evaluation of the cytotoxicity of EBM-SeNPs on lung cancer cells and normal liver cells. **A.** Heat map of the B-SeNPs, EBM, and EBM-SeNPs inhibition rates at different concentrations on A549 cells. **B.** Heat map of the B-SeNPs, EBM, and EBM-SeNPs survival rates at different concentrations on L-02 cells. DDP (5 ug/ml) was used as a positive control.

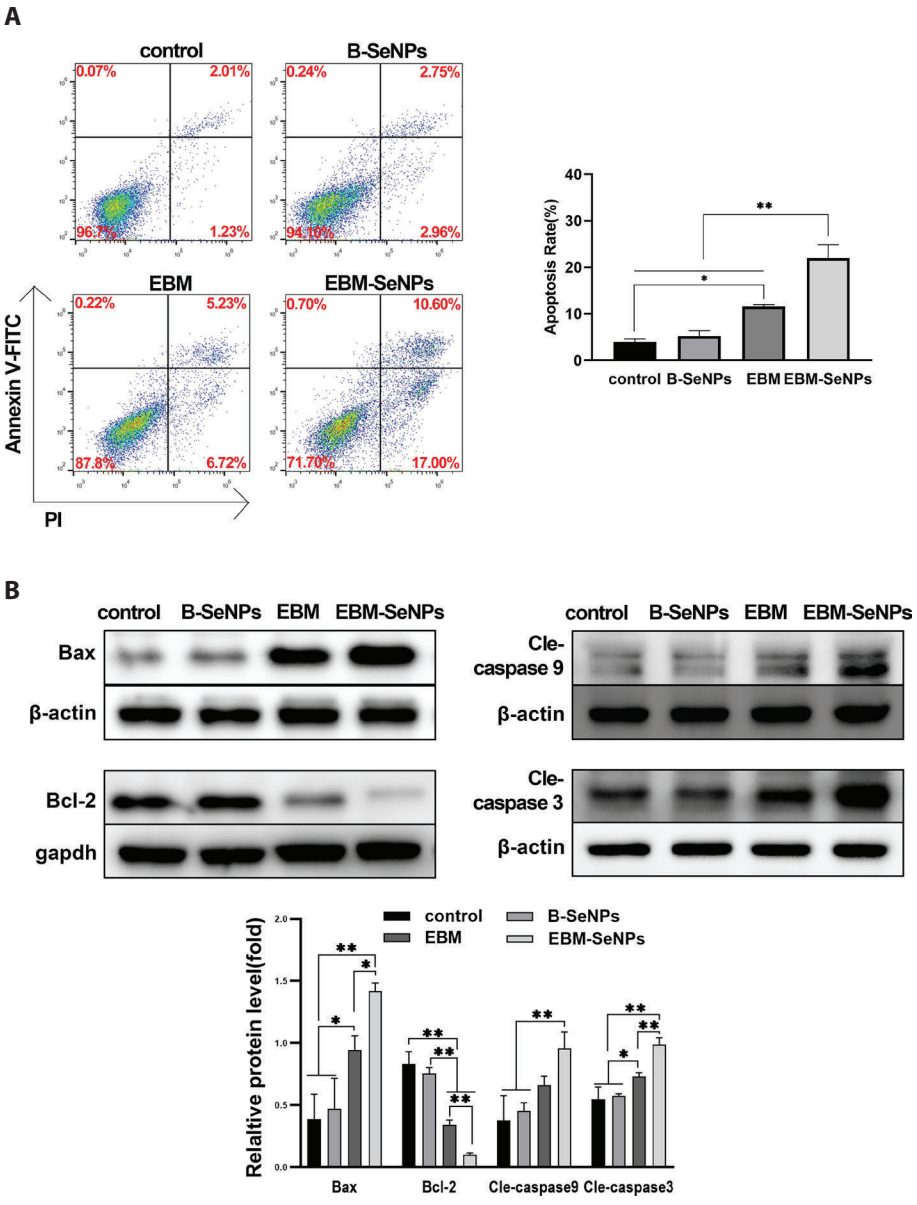

Figure 4. The detection of cellular apoptosis. **A.** The apoptotic effect of B-SeNPs, EBM, and EBM-SeNPs on A549 cells detected by flow cytometry. **B.** The protein expression of SeNPs, EBM, and EBM-SeNPs on A549 cells detected by Western blot. * $p < 0.05$, ** $p < 0.01$.

apoptotic induction ability of EBM-SeNPs was significantly enhanced compared to that of EBM.

Antiapoptotic protein Bcl-2 is one of the primary regulators of apoptosis (Dong et al. 2016; Singh et al. 2019). Bax, a pro-apoptotic protein, is capable of forming heterodimers with Bcl-2, thus facilitating apoptosis (Liu et al. 2015). The pro-apoptosis effect of the EBM-SeNPs was further verified by the detection of Bcl-2 and Bax. The results demonstrated that the treatment of EBM and EBM-SeNPs considerably increased Bax expression and decreased Bcl-2 expression (Fig. 4B), suggesting that, consistent with the results of flow cytometry, EBM-SeNPs had a stronger effect on inducing Bax expression and inhibiting Bcl-2 expression than EBM. Caspase-3, an essential apoptosis executor, can be stimulated by caspase-9 and other initiators, which is capable of causing cell apoptosis *via* cleavage of numerous cellular substrates (Chen et al. 2008; Pfeffer and Singh 2018). Results of Western blot demonstrated that EBM-SeNPs considerably upregulated the expression of Cleaved-caspase 3 and Cleaved-caspase 9. Therefore, EBM-SeNPs may induce apoptosis in A549 cells by regulate the expression of Bax, Bcl-2 and caspase 3.

Inhibitory effect of EBM-SeNPs on A549 cells growth

The cell cycle is crucial for cell growth (Ramadoss and Sivalingam 2021). As shown in Figure 5A, a flow cytometry analysis

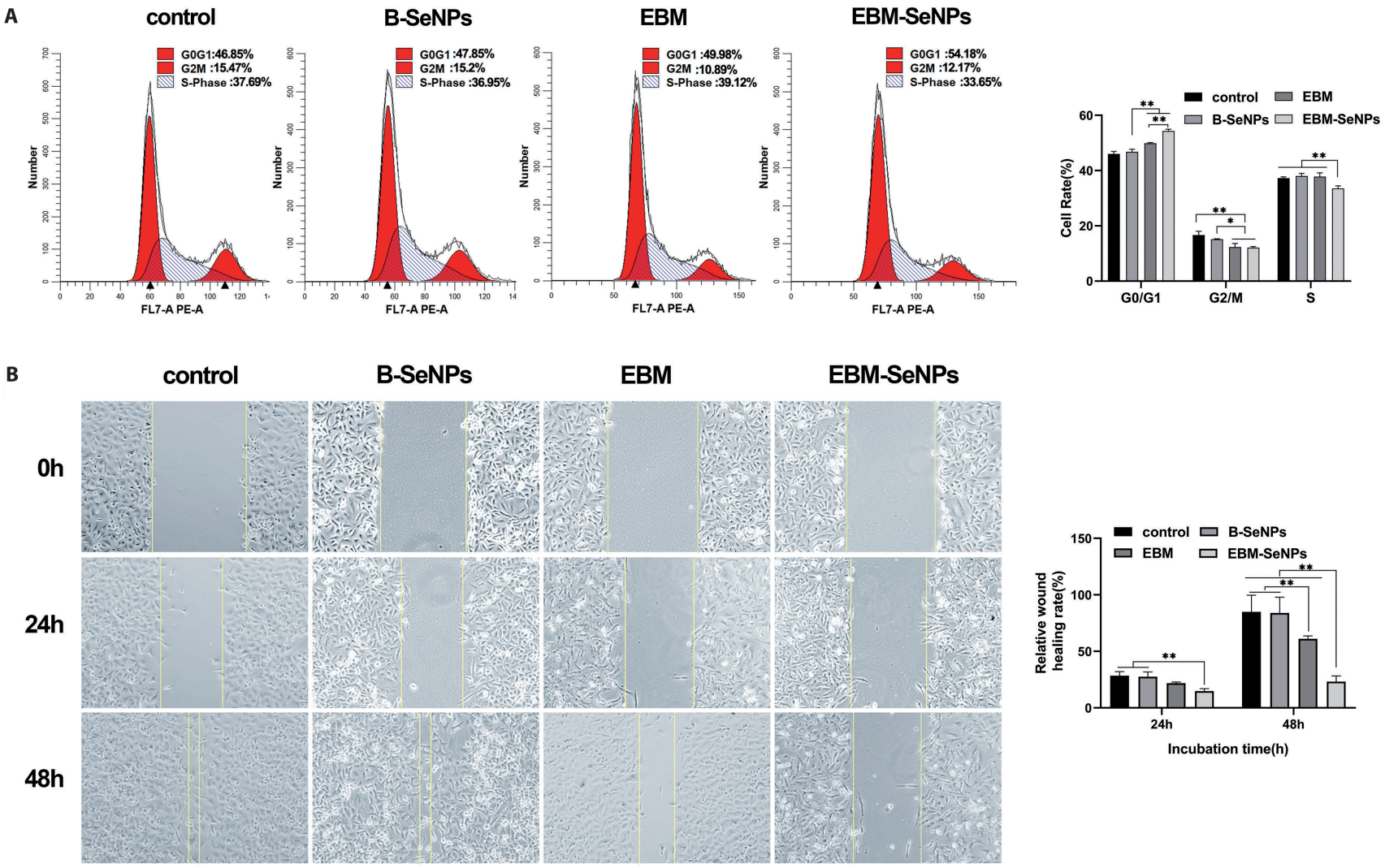

Figure 5. Cell cycle analysis and Wound healing assay. **A.** The cell cycle analysis of A549 cells treated with B-SeNPs, EBM, and EBM-SeNPs. **B.** Wound-healing assay image and relative migration rate of each group on A549 cells. * $p < 0.05$, ** $p < 0.01$ *vs.* control group.

was performed to examine the effect of EBM-SeNPs on the cell cycle of A549 cells. The results showed that, in comparison with the control group, both EBM-SeNPs and EBM significantly increased the proportion of cells in G0/G1 phase, indicating the ability of EBM-SeNPs and EBM to induce cell cycle arrest at this stage. Furthermore, the percentage of cells in G0/G1 phase was notably higher in the EBM-SeNPs group compared to the EBM group, suggesting a stronger inhibitory effect of EBM-SeNPs on A549 cells in cell cycle. Conversely, B-SeNPs exhibited negligible impact on cell cycle due to inherent structural instability. These findings demonstrated that EBM-SeNPs effectively arrested the cell cycle of lung cancer cells in the G0/G1 phase, highlighting the essential role of EBM-mediated modification in enhancing the biological activity of SeNPs.

Inhibitory effect of EBM-SeNPs on A549 cells migration

The ability of cell migration plays a crucial role in tumor metastasis (Kramer et al. 2013). A Wound healing assay was conducted to further examine the effect of EBM-SeNPs on the migration of A549 cells (Fig. 5B). Compared to the control group, both the EBM and EBM-SeNPs groups exhibited significantly lower migration rates, indicating their significant inhibition on A549 cell migration *in vitro*. Notably, the inhibitory effect of EBM-SeNPs was evident as early as 24 h after drug treatment, whereas no such phenomenon was observed in the EBM group. Furthermore, the wound healing rate of the EBM-SeNPs group was significantly lower than that of the EBM group, highlighting a much stronger inhibitory effect of EBM-SeNPs on A549 cells compared to EBM alone. As anticipated, B-SeNPs had minimal impact on cell migration.

Antitumor effect of EBM-SeNPs in vivo

Tumor volume

To further confirm the anti-lung cancer effects of EBM-SeNPs *in vivo*, we evaluated the efficacy of EBM-SeNPs

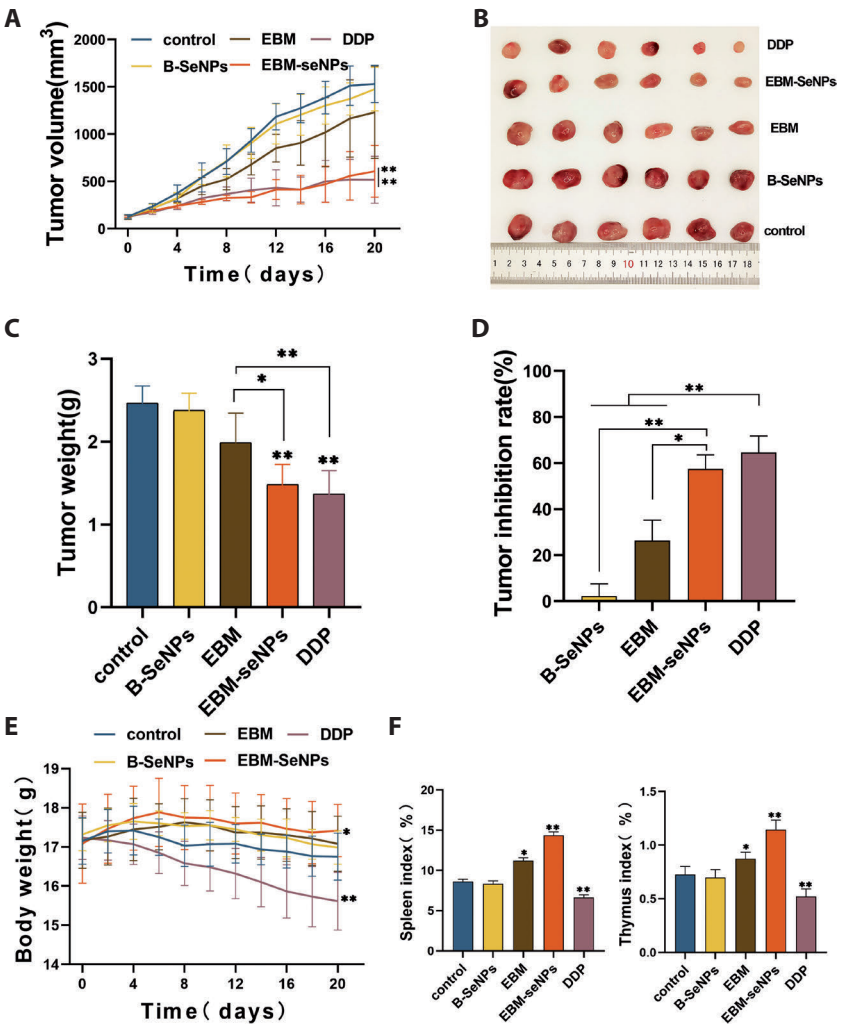

Figure 6. Antitumor effects of B-SeNPs, EBM, and EBM-SeNPs on LLC tumor-bearing mice. **A.** Changes in tumor volume among mice over the three weeks. **B.** Photograph of tumors from different groups. **C.** The tumor weight of mice. **D.** The tumor inhibition rate under various treatment regimens. **E.** The temporal progression of body weights in mice. **F.** Spleen and thymus index in different groups. * $p < 0.05$, ** $p < 0.01$ *vs.* control group.

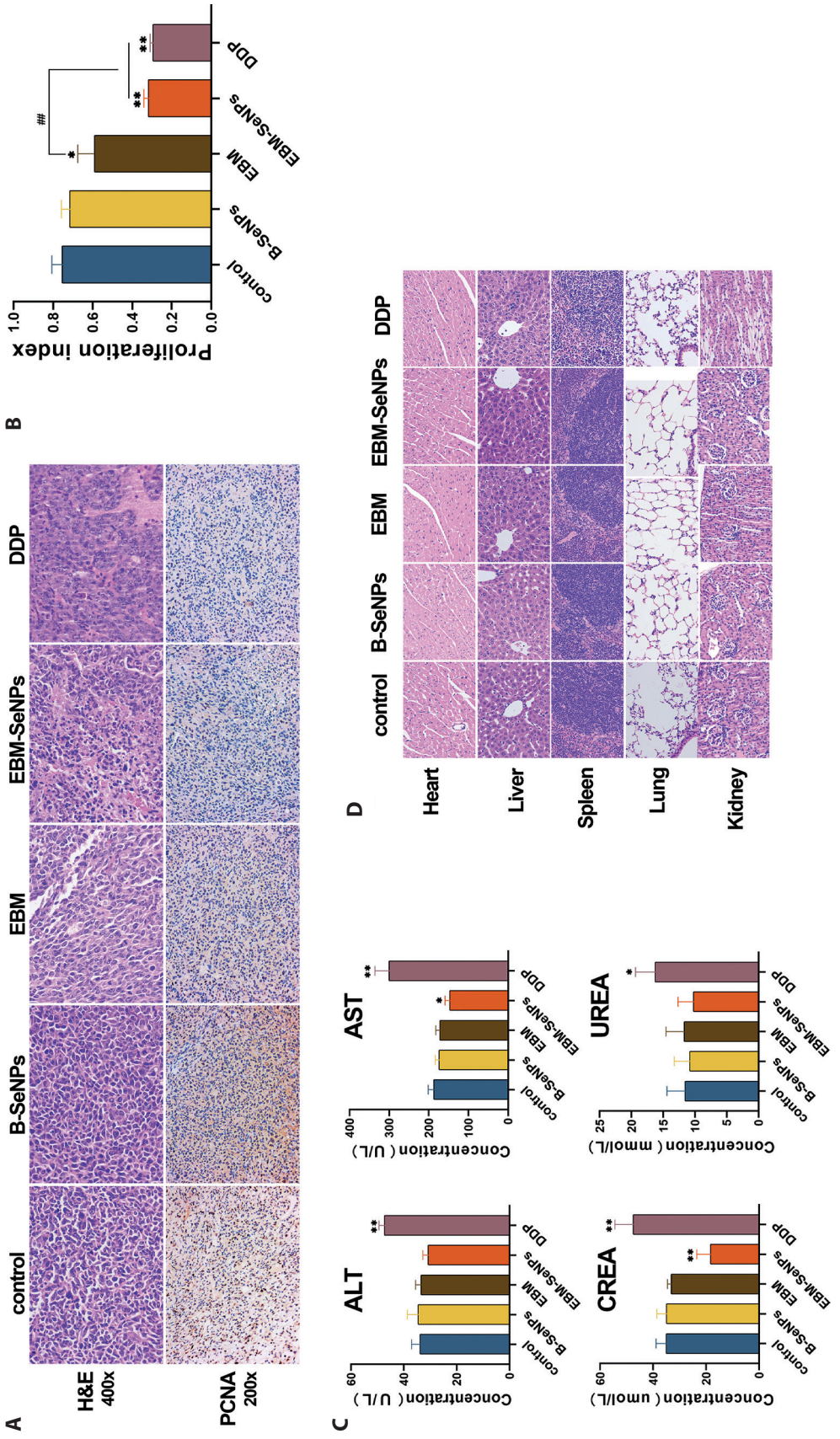

Figure 7. H&E and Immunohistochemical analysis of tumor tissue and Bio-safety of EBM-SeNPs. **A.** H&E, PCNA staining of tumor in each group. **B.** Proliferative index in different groups. **C.** Blood biochemistry analysis of ALT, AST, CREA, and UREA in each group. **D.** H&E staining images of heart, liver, spleen, lung, and kidney in each group (magnification 400×). * $p < 0.05$, ** $p < 0.01$ *vs.* control group.

in C57BL/6 mice bearing tumors derived from LLC cells. Figure 6A portrayed the trend for change in the tumor size. After the treatment of 21 days, the tumors were excised, photographed (Fig. 6B) and weighed for calculation of the inhibition rate (Fig. 6C,D). Consistent with the results *in vitro*, tumor volume curves and tumor weight of mice in the EBM-SeNPs and DDP group exhibited a significantly lower level compared to that in the control group, indicating that EBM-SeNPs has a similar anti-tumor effect as DDP *in vivo*. It is noteworthy that there was no statistically significant difference in tumor volume and tumor weight between the EBM group and control group, which may be attributed to reduced bioavailability of EBM *in vivo*.

Body weight and immune organ index

The body weight of mice can reflect the toxicity of drugs to a certain extent. The body weight of mice in each group was monitored over 21 days (Fig. 6E). The weight of mice in the B-SeNPs, EBM, EBM-SeNPs, and control group remained stable throughout the administration period, indicating that these drugs did not cause any significant toxicity to mice. In contrast, mice treated with DDP experienced significant weight loss due to potential gastrointestinal reactions and hepatorenal toxicity (Shahid et al. 2018; Qi et al. 2019). It is worth mentioning that the weight curve of mice in the EBM-SeNPs group was located above that of the control group, suggesting that EBM-SeNPs may confer protective effects in mice at the current drug dosage. These findings may be attributed to the regulation of intestinal absorption, immune enhancement, and detoxification by EBM-SeNPs (Chen et al. 2022).

Considering the recognition that immune organ index are significant indicators of immune functions. The examination of the thymus and spleen index in treatment groups were conducted (Ding et al. 2019). Figure 6F showed that the thymus and spleen index of mice in EBM group and EBM-SeNPs group of mice demonstrated an increase, with the EBM-SeNPs group showing a more significant effect on immune organ index, which can be ascribed to the synergistic interaction between EBM and SeNPs (Razaghi et al. 2021). Conversely, the thymus and spleen index of mice in DDP group exhibited a decrease, which may be ascribed to the prominent immunosuppressive adverse effects associated with DDP (Qi et al. 2019).

H&E and immunohistochemical analysis

Tumor tissues were stained with H&E and PCNA to further elucidate the antitumor activity of EBM-SeNPs. The results of H&E staining indicated a higher incidence of cell necrosis and karyopyknosis in the EBM-SeNPs and DDP groups, compared to the control group (Fig. 7A). The number of PCNA positive cells in EBM-SeNPs and DDP groups also decreased significantly in comparison to the control group, indicating a decline in tumor proliferation (Fig. 7B). These histological results indicated that EBM-SeNPs had stronger anti-lung cancer activity than NS, B-SeNPs and EBM groups which was consistent with the previous results.

Biocompatibility analysis in vivo

Routine blood biochemical parameters were assessed to evaluate the biocompatibility of EBM-SeNPs. As

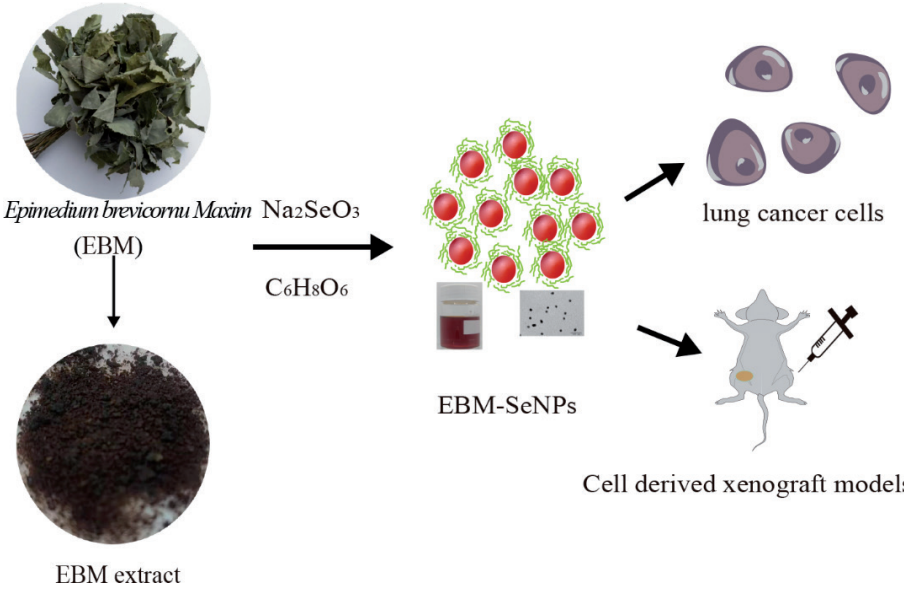

Figure 8. Summary of the synthesis of *Epimedium* selenium nanoparticles and efficacy against cancer.

demonstrated in Figure 7C, the serum levels of ALT, AST, UREA, and CREA in the B-SeNPs, EBM, and EBM-SeNPs groups were all within the normal range, indicating no evidence of liver or kidney dysfunction (Dicson et al. 2015). The mice in DDP group, however, exhibited significant hepatic and renal impairment, consistent with previous investigations (Qi et al. 2019). Interestingly, both AST and CREA levels of mice in EBM-SeNPs group exhibited a significant decrease compared to those in the control group, indicating a protective effect on liver and kidney function (Abu-Zeid et al. 2021; Al-Brakati et al. 2021). The results were further validated through H&E staining of vital internal organs (heart, liver, spleen, lung, and kidney). As depicted in Figure 7D, the B-SeNPs, EBM, and EBM-SeNPs groups exhibited no apparent signs of organ toxicity, while conspicuous vacuolar degeneration was observed in the kidney specimens from the DDP group.

Discussion

The physicochemical properties and efficiency against lung cancer of EBM-SeNPs was evaluated in this study. The successful synthesis of EBM-SeNPs using *Epimedium brevicornum Maxim* extract with an average diameter of 65 nm was reported. The physicochemical properties of EBM-SeNPs were analyzed by UV-vis spectroscopy, TEM, FT-IR, EDX and ICP-OES. EBM-SeNPs can promote lung cancer cell apoptosis, and inhibit growth and migration of lung cancer cells, hence indicating a stronger anti-tumor effect compared with B-SeNPs and EBM *in vitro*. Furthermore, the results *in vivo* proved that EBM-SeNPs were safe and biocompatible as they decreased tumor volume and weight while increasing the immune organ index in tumor-bearing mice. In summary, EBM-SeNPs derived from *Epimedium brevicornum Maxim* extract have the potential to be used as a novel antitumor agent against lung cancer (Fig. 8).

Nanoparticles are known to induce strong oxidative stress *in vivo* and *in vitro* because of intracellular reactive oxygen species (ROS) generation. The oxidative stress triggered by nanoparticle has been associated with lung inflammation and injury. It has been reported that ascorbic acid, a water-soluble radical scavenger, could inhibit intracellular oxidative stress induced by nanoparticles (Fukui et al. 2017). The treatment of ascorbic acid would be a solution to the potential drug toxicity of selenium nanomedicine.

Conflict of interests. The authors declared no competing financial interests.

Ethics statement. All animal experiments were approved by the Institutional Animal Care and Use Committee of the Second Affiliated Hospital of Chongqing Medical University (approval number: IACUC- SAHCQMU-2023-0021).

Funding. This study was supported by grants from Kuanren Elite Backbone Talents Special project of the Second Affiliated Hospital of Chongqing Medical University (KY2019G007).

Acknowledgements. Firstly, I would like to extend my heartfelt appreciation to Professor Tong Jin, my supervisor, for her invaluable guidance throughout the duration of this experiment. Secondly, I wish to acknowledge the support provided by the Kuanren Elite Backbone Talents Special Fund in facilitating this research endeavor.

References

Abu-Zeid EH, Abdel Fattah DM, Arisha AH, Ismail TA, Alsadek DM, Metwally MMM, El-Sayed AA, Khalil AT (2021): Protective prospects of eco-friendly synthesized selenium nanoparticles using Moringa oleifera or Moringa oleifera leaf extract against melamine induced nephrotoxicity in male rats. Ecotoxicol. Environ. Saf. **221,** 112424 https://doi.org/10.1016/j.ecoenv.2021.112424

Adam-Dima EI, Balas M, Anastasescu M, Purdel C, Margină D (2024): Synthesis of homogeneous spherical selenium nanoparticles through a chemical method for cancer therapy applications. Toxicol. In Vitro **95,** 105765 https://doi.org/10.1016/j.tiv.2023.105765

Al-Brakati A, Alsharif KF, Alzahrani KJ, Kabrah S, Al-Amer O, Oyouni AA, Habotta OA, Lokman MS, Bauomy AA, Kassab RB, Abdel Moneim AE (2021): Using green biosynthesized lycopene-coated selenium nanoparticles to rescue renal damage in glycerol-induced acute kidney injury in rats. Int. J. Nanomedicine **16,** 4335-4349 https://doi.org/10.2147/IJN.S306186

Almukainzi M, El-Masry TA, Selim H, Saleh A, El-Sheekh M, Makhlof MEM, El-Bouseary MM (2023): New insight on the cytoprotective/antioxidant pathway Keap1/Nrf2/HO-1 modulation by ulva intestinalis extract and its selenium nanoparticles in rats with carrageenan-induced paw edema. Mar. Drugs **21,** 459 https://doi.org/10.3390/md21090459

Bade BC, Dela Cruz CS (2020): Lung cancer 2020: Epidemiology, etiology, and prevention. Clin. Chest Med. **41,** 1-24 https://doi.org/10.1016/j.ccm.2019.10.001

Cao BL, Zhang Q, Guo J, Guo RX, Fan XD, Bi YG (2021): Synthesis and evaluation of polysaccharides-functionalized selenium nanoparticles. Int. J. Biol. Macromol. **191,** 832-839 https://doi.org/10.1016/j.ijbiomac.2021.09.087

Chen JH, Cao JL, Chu YL, Wang ZL, Yang ZT, Wang HL (2008): T-2 toxin-induced apoptosis involving Fas, p53, Bcl-xL, Bcl-2, Bax and caspase-3 signaling pathways in human chondrocytes. J. Zhejiang Univ. Sci. B **9,** 455-463 https://doi.org/10.1631/jzus.B0820013

Chen N, Yao P, Zhang W, Zhang Y, Xin N, Wei H, Zhang T, Zhao C (2022): Selenium nanoparticles: Enhanced nutrition and beyond. Crit. Rev. Food Sci. Nutr. **63,** 12360-12371 https://doi.org/10.1080/10408398.2022.2101093

Chen Y, Xia H, Zhong X (2024): In Vitro evaluation of the anti-pancreatic cancer activity of epimedium herb. Front. Pharmacol. **15,** 1389221
https://doi.org/10.3389/fphar.2024.1389221

Dicson SM, Samuthirapandi M, Govindaraju A, Kasi PD (2015): Evaluation of in vitro and in vivo safety profile of the Indian traditional medicinal plant Grewia tiliaefolia. Regul. Toxicol. Pharmacol. **73,** 241-247
https://doi.org/10.1016/j.yrtph.2015.07.011

Ding Y, Yan YM, Chen D, Ran LW, Mi J, Lu L, Jing B, LiX, Zeng X, Cao Y (2019): Modulating effects of polysaccharides from the fruits of Lycium barbarum on the immune response and gut microbiota in cyclophosphamide-treated mice. Food Funct. **10,** 3671-3683
https://doi.org/10.1039/C9FO00638A

Dogaru CB, Duță C, Muscurel C, Stoian I (2023): „Alphabet" selenoproteins: Implications in pathology. Int. J. Mol. Sci. **24,** 15344
https://doi.org/10.3390/ijms242015344

Dong YC, Zheng YJ, Xiao J, Zhu C, Zhao MS (2016): Regulatory effect of Bcl-2 in ultraviolet radiation-induced apoptosis of the mouse crystalline lens. Exp. Ther. Med. **11,** 973-977
https://doi.org/10.3892/etm.2015.2960

Fu A, Yao B, Dong T, Chen Y, Yao J, Liu Y, Li H, Bai H, Liu X, Zhang Y (2022): Tumor-resident intracellular microbiota promotes metastatic colonization in breast cancer. Cell **185,** 1356-1372.e26
https://doi.org/10.1016/j.cell.2022.02.027

Fukui H, Iwahashi H, Nishio K, Hagihara Y, Yoshida Y, Horie M (2017): Ascorbic acid prevents zinc oxide nanoparticle-induced intracellular oxidative stress and inflammatory responses. Toxicol. Ind. Health **33,** 687-695
https://doi.org/10.1177/0748233717707361

Gu ZF, Zhang ZT, Wang JY, Xu BB (2017): Icariin exerts inhibitory effects on the growth and metastasis of KYSE70 human esophageal carcinoma cells via PI3K/AKT and STAT3 pathways. Environ. Toxicol. Pharmacol. **54,** 7-13
https://doi.org/10.1016/j.etap.2017.06.004

Gunti L, Dass RS, Kalagatur NK (2019): Phytofabrication of selenium nanoparticles from fruit extract and exploring its biopotential applications: antioxidant, antimicrobial, and biocompatibility. Front. Microbiol. **10,** 931
https://doi.org/10.3389/fmicb.2019.00931

Haji Mehdi Nouri Z, Tafvizi F, Amini K, Khandandezfully N, Kheirkhah B (2024): Enhanced induction of apoptosis and cell cycle arrest in MCF-7 breast cancer and HT-29 colon cancer cell lines via low-dose biosynthesis of selenium nanoparticles utilizing lactobacillus casei. Biol. Trace Elem. Res. **202,** 1288-1304
https://doi.org/10.1007/s12011-023-03738-5

Hassan FAS, Ali EF, Mostafa NY, Mazrou R (2021): Shelf-life extension of sweet basil leaves by edible coating with thyme volatile oil encapsulated chitosan nanoparticles. Int. J. Biol. Macromol. **177,** 517-525
https://doi.org/10.1016/j.ijbiomac.2021.02.159

Hernández-Díaz JA, Garza-García JJ, León-Morales JM, Zamudio-Ojeda A, Arratia-Quijada J, Velázquez-Juárez G, López-Velázquez JC, García-Morales S (2021): Antibacterial activity of biosynthesized selenium nanoparticles using extracts of calendula officinalis against potentially clinical bacterial strains. Molecules **26,** 5929
https://doi.org/10.3390/molecules26195929

Huong QTT, Nguyen N, Duy BT, Hoang A, Hai ND, Ngan HTK, Ngan LT, Nhi TLH, Linh DTY, Khanh TN (2023): Structurally natural chitosan films decorated with extract and selenium nanoparticles: Properties and strawberry preservation. Food Bioscience **53,** 102647
https://doi.org/10.1016/j.fbio.2023.102647

Jiang J, Jiang L, Maldonato BJ, Wang Y, Holderfield M, Aronchik I, Winters IP, Salman Z, Blaj C, Menard M, et al. (2024): Translational and therapeutic evaluation of RAS-GTP inhibition by RMC-6236 in RAS-driven cancers. Cancer Discov. **14,** 994-1017
https://doi.org/10.1158/2159-8290.CD-24-0027

Ke LT, Duan XQ, Cui J, Song XP, Ma WR, Zhang WM, Liu Y, Fan Y (2023): Research progress on the extraction technology and activity study of Epimedium polysaccharides. Carbohyd. Polym. **306,** 120602
https://doi.org/10.1016/j.carbpol.2023.120602

Kramer N, Walzl A, Unger C, Rosner M, Krupitza G, Hengstschlager M, Dolznig H (2013): In vitro cell migration and invasion assays. Mutat. Res. **752,** 10-24
https://doi.org/10.1016/j.mrrev.2012.08.001

Lahiri A, Maji A, Potdar PD, Singh N, Parikh P, Bisht B, Mukherjee A, Paul MK (2023): Lung cancer immunotherapy: progress, pitfalls, and promises. Mol. Cancer **22,** 40
https://doi.org/10.1186/s12943-023-01740-y

Li P, Liu Y, Faraone JN, Hsu CC, Chamblee M, Zheng YM, Carlin C, Bednash JS, Horowitz JC, Mallampalli RK (2024): Distinct patterns of SARS-CoV-2 BA.2.87.1 and JN.1 variants in immune evasion, antigenicity, and cell-cell fusion. MBio **5,** e0075124
https://doi.org/10.1128/mbio.00751-24

Li SL, Xu SS, Liang XY, Xue YG, Mei J, Ma YF, Liu Y, Liu Y (2021): Nanotechnology: breaking the current treatment limits of lung cancer. Adv. Healthc. Mater. **10,** e2100078
https://doi.org/10.1002/adhm.202100078

Liu FY, Ding DN, Wang YR, Liu SX, Peng C, Shen F, Zhu XY, Li C, Tang LP, Han FJ (2023): Icariin as a potential anticancer agent: a review of its biological effects on various cancers. Front. Pharmacol. **14,** 1216363
https://doi.org/10.3389/fphar.2023.1216363

Liu Q, Si TL, Xu XY, Liang FQ, Wang LF, Pan SY (2015): Electromagnetic radiation at 900 MHz induces sperm apoptosis through bcl-2, bax and caspase-3 signaling pathways in rats. Reprod. Health **12,** 65
https://doi.org/10.1186/s12978-015-0062-3

Liu Y, Yang LT, Long WJ, Wang LJ, Wang ZH (2020): Medication rules of traditional Chinese medicine for the treatment of premature ejaculation: An analysis based on data mining. Zhonghua Nan Ke Xue **26,** 650-655 (in Chinese)

Liu YM, Li XQ, Zhang XR, Chen YY, Liu YP, Zhang HQ, Chen Y (2023): Uncovering the key pharmacodynamic material basis and possible molecular mechanism of extract of Epimedium against liver cancer through a comprehensive investigation. J. Ethnopharmacol. **317,** 116765
https://doi.org/10.1016/j.jep.2023.116765

Lu X, Xue B, Zhang T, Zhou X, Zhang Y (2019): Down-regulation of microRNA-10a mediates the anti-tumor effect of icaritin in A549 cells via the PTEN/AKT and ERK pathway. Gen. Physiol. Biophys. **38,** 525-533 https://doi.org/10.4149/gpb_2019041

Lu Y, Gao Y, Yang H, Hu Y, Li X (2022): Nanomedicine-boosting icaritin-based immunotherapy of advanced hepatocellular carcinoma. Milit. Med. Res. **9,** 69 https://doi.org/10.1186/s40779-022-00433-9

Luo P, An Y, He J, Xing X, Zhang Q, Liu X, Chen Y, Yuan H, Chen J, Wong YK, et al. (2024): Icaritin with autophagy/mitophagy inhibitors synergistically enhances anticancer efficacy and apoptotic effects through PINK1/Parkin-mediated mitophagy in hepatocellular carcinoma. Cancer Lett. **587,** 216621 https://doi.org/10.1016/j.canlet.2024.216621

Luo Z, Liu X, Chen Y, Shen L, Qin H, Zha Q, Hu F, Wang Y (2024): Gene features of tumor-specific T cells relevant to immunotherapy, targeted therapy and chemotherapy in lung cancer. Heliyon **10,** e28374 https://doi.org/10.1016/j.heliyon.2024.e28374

Maia LB, Maiti BK, Moura I, Moura JJG (2023): Selenium-more than just a fortuitous sulfur substitute in redox biology. Molecules **29,** 120 https://doi.org/10.3390/molecules29010120

Manjunatha C, Rao PP, Bhardwaj P, Raju H, Ranganath D (2021): New insight into the synthesis, morphological architectures and biomedical applications of elemental selenium nanostructures. Biomed. Mater. **16,** 022010

Martínez-Esquivias F, Gutiérrez-Angulo M, Pérez-Larios A, Sánchez-Burgos JA, Becerra-Ruiz JS, Guzmán-Flores JM (2022): Anticancer activity of selenium nanoparticles studies. Anticancer Agents Med. Chem. **22,** 1658-1673 https://doi.org/10.2174/1871520621666210910084216

Menon S, Jayakodi S, Yadav KK, Somu P, Isaq M, Shanmugam VK, Chaitanyakumar A, Basavegowda N (2022): Preparation of paclitaxel-encapsulated bio-functionalized selenium nanoparticles and evaluation of their efficacy against cervical cancer. Molecules **27,** 7290 https://doi.org/10.3390/molecules27217290

Mikhailova EO (2023): Selenium nanoparticles: green synthesis and biomedical application. Molecules **28,** 8125 https://doi.org/10.3390/molecules28248125

Naseer S, Lone SH, Lone JA, Khuroo MA, Bhat KA (2015): LC-MS guided isolation, quantification and antioxidant evaluation of bioactive principles from Epimedium elatum. J. Chromatogr. B Analyt. Technol. Biomed. Life Sci. **989,** 62-70 https://doi.org/10.1016/j.jchromb.2015.02.046

Nasir A, Bullo MMH, Ahmed Z, Imtiaz A, Yaqoob E, Jadoon M, Ahmed H, Afreen A, Yaquoob S (2020): Nutrigenomics: Epigenetics and cancer prevention: A comprehensive review. Crit. Rev. Food Sci. Nutr. **60,** 1375-1387 https://doi.org/10.1080/10408398.2019.1571480

Oliver AL (2022): Lung cancer epidemiology and screening. Surg. Clin. North Am. **102,** 335-344 https://doi.org/10.1016/j.suc.2021.12.001

Pfeffer CM, Singh ATK (2018): Apoptosis: A target for anticancer therapy. Int. J. Mol. Sci. **19,** 448 https://doi.org/10.3390/ijms19020448

Qi L, Luo Q, Zhang Y, Jia F, Zhao Y, Wang F (2019): Advances in toxicological research of the anticancer drug cisplatin. Chem. Res. Toxicol. **32,** 1469-1486 https://doi.org/10.1021/acs.chemrestox.9b00204

Ramadoss DP, Sivalingam N (2021): Vanillin extracted from proso and barnyard millets induces cell cycle inhibition and apoptotic cell death in MCF-7 cell line. J. Cancer Res. Ther. **17,** 1425-1433 https://doi.org/10.4103/jcrt.JCRT_1128_19

Razaghi A, Poorebrahim M, Sarhan D, Björnstedt M (2021): Selenium stimulates the antitumour immunity: Insights to future research. Eur. J. Cancer **155,** 256-267 https://doi.org/10.1016/j.ejca.2021.07.013

Rong TX, Yue ZM, Hua L, Xiang LZ, Xiao SJ, University J (2015): Morphological and anatomy studies on after-ripening seeds of epimedium sagittatum maxim. Seed

Sampath S, Sunderam V, Manjusha M, Dlamini Z, Lawrance AV (2024): Selenium nanoparticles: a comprehensive examination of synthesis techniques and their diverse applications in medical research and toxicology studies. Molecules **29,** 801 https://doi.org/10.3390/molecules29040801

Schabath MB, Cote ML (2019): Cancer progress and priorities: Lung cancer. Cancer Epidem. Biomar. **28,** 1563-1579 https://doi.org/10.1158/1055-9965.EPI-19-0221

Sha M, Cao A, Yang S, Xue Y (1997): Determination of icariin in Epimedium koreanum nakai by high performance liquid chromatography. Se Pu (Chinese journal of chromatography) **15,** 166-167 (in Chinese)

Shahid F, Farooqui Z, Khan F (2018): Cisplatin-induced gastrointestinal toxicity: An update on possible mechanisms and on available gastroprotective strategies. Eur. J. Pharmacol. **827,** 49-57 https://doi.org/10.1016/j.ejphar.2018.03.009

Shi XD, Tian YQ, Wu JL, Wang SY (2021): Synthesis, characterization, and biological activity of selenium nanoparticles conjugated with polysaccharides. Crit. Rev. Food Sci. Nutr. **61,** 2225-2236 https://doi.org/10.1080/10408398.2020.1774497

Singh H, Kaur J, Datusalia AK, Naqvi S (2024): Age-dependent assessment of selenium nanoparticles: biodistribution and toxicity study in young and adult rats. Nanomedicine (Lond.) **27,** 2021-2038 https://doi.org/10.2217/nnm-2023-0204

Singh R, Letai A, Sarosiek K (2019): Regulation of apoptosis in health and disease: the balancing act of BCL-2 family proteins. Nat. Rev. Mol. Cell Bio. **20,** 175-193 https://doi.org/10.1038/s41580-018-0089-8

Song J, Shu L, Zhang Z, Tan X, Sun E, Jin X, Chen Y, Jia X (2012): Reactive oxygen species-mediated mitochondrial pathway is involved in Baohuoside I-induced apoptosis in human non-small cell lung cancer. Chem. Biol. Interact. **199,** 9-17 https://doi.org/10.1016/j.cbi.2012.05.005

Tong X, Wang Y, Dong BC, Li Y, Lang S, Ma JX, Ma XL (2023): Effects of genus in the treatment of osteoarthritis and relevant signaling pathways. Chin. Med. **18,** 92 https://doi.org/10.1186/s13020-023-00788-8

Urbankova L, Skalickova S, Pribilova M, Ridoskova A, Pelcova P, Skladanka J, Horky P (2021): Effects of sub-lethal doses

of selenium nanoparticles on the health status of rats. Toxics **9,** 28
https://doi.org/10.3390/toxics9020028

Veeraraghavan VP, Periadurai ND, Karunakaran T, Hussain S, Surapaneni KM, Jiao X (2021): Green synthesis of silver nanoparticles from aqueous extract of Scutellaria barbata and coating on the cotton fabric for antimicrobial applications and wound healing activity in fibroblast cells (L929). Saudi J. Biol. Sci. **28,** 3633-3640
https://doi.org/10.1016/j.sjbs.2021.05.007

Vu LVK, Tran NTT, Duy NN, Nguyen TTL, Dinh TP (2023): Application of electron beam irradiation for selenium nanoparticles production using gum Arabic as stabilizer. Radiation Physics and Chemistry **211,** 111061
https://doi.org/10.1016/j.radphyschem.2023.111061

Vundela SR, Kalagatur NK, Nagaraj A, Kadirvelu K, Chandranayaka S, Kondapalli K, Hashem A, Abd Allah EF, Poda S (2021): Multi-biofunctional properties of phytofabricated selenium nanoparticles from carica papaya fruit extract: antioxidant, antimicrobial, antimycotoxin, anticancer, and biocompatibility. Front. Microbiol. **12,** 769891
https://doi.org/10.3389/fmicb.2021.769891

Wang L, Li C, Huang Q, Fu X (2019): Biofunctionalization of selenium nanoparticles with a polysaccharide from Rosa roxburghii fruit and their protective effect against H2O2-induced apoptosis in INS-1 cells. Food Funct. **10,** 539-553
https://doi.org/10.1039/C8FO01958D

Wang L, Periyasami G, Aldalbahi A, Fogliano V (2021): The antimicrobial activity of silver nanoparticles biocomposite films depends on the silver ions release behaviour. Food Chem. **359,** 129859
https://doi.org/10.1016/j.foodchem.2021.129859

Yan JK, Qiu WY, Wang YY, Wang WH, Yang Y, Zhang HN (2018): Fabrication and stabilization of biocompatible selenium nanoparticles by carboxylic curdlans with various molecular properties. Carbohyd. Polym. **179,** 19-27
https://doi.org/10.1016/j.carbpol.2017.09.063

Yang Z, Hu Y, Yue P, Li H, Wu Y, Hao X, Peng F (2023): Structure, stability, antioxidant activity, and controlled-release of selenium nanoparticles decorated with lichenan from Usnea longissima. Carbohydr. Polym. **299,** 120219
https://doi.org/10.1016/j.carbpol.2022.120219

Zhang L, Zeng HW, Cheng WH (2018): Beneficial and paradoxical roles of selenium at nutritional levels of intake in healthspan and longevity. Free Radic. Biol. Med. **127,** 3-13
https://doi.org/10.1016/j.freeradbiomed.2018.05.067

Zhang X, Tang B, Wen S, Wang Y, Pan C, Qu L, Yin Y, Wei Y (2023a): Advancements in the biotransformation and biosynthesis of the primary active flavonoids derived from epimedium. Molecules **28,** 7173
https://doi.org/10.3390/molecules28207173

Zhang X, Xiao YD, Huang QL (2023b): The cellular uptake of exopolysaccharide-selenium nanoparticles and their induced apoptosis of HepG2 cells mitochondria- and death receptor-mediated pathways. Int. J. Biol. Macromol. **247,** 125747
https://doi.org/10.1016/j.ijbiomac.2023.125747

Zhang Y, Li J, Wang Y, Liang Q (2022): Taxonomy of Epimedium (Berberidaceae) with special reference to Chinese species. Chin. Herb. Med. **14,** 20-35
https://doi.org/10.1016/j.chmed.2021.12.001

Zhang ZH, Du YX, Liu T, Wong KH, Chen TF (2019): Systematic acute and subchronic toxicity evaluation of polysaccharide-protein complex-functionalized selenium nanoparticles with anticancer potency. Biomater. Sci. **7,** 5112-5123
https://doi.org/10.1039/C9BM01104H

Zhao HS, Shan YH, Ma Z, Yu MW, Gong BJ (2019): A network pharmacology approach to explore active compounds and pharmacological mechanisms of epimedium for treatment of premature ovarian insufficiency. Drug Des. Devel. Ther. **13,** 2997-3007
https://doi.org/10.2147/DDDT.S207823

Zhou LA, Song ZT, Zhang SJ, Li YL, Xu J, Guo YQ (2021): Construction and antitumor activity of selenium nanoparticles decorated with the polysaccharide extracted from Citrus limon (L.) Burm. f. (Rutaceae). Int. J. Biol. Macromol. **188,** 904-913
https://doi.org/10.1016/j.ijbiomac.2021.07.142

Zhu J, Liu Z, Pu Y, Xu J, Zhang S, Bao Y (2022): Green synthesized gold nanoparticles from Pseudobulbus Cremastrae seu Pleiones show efficacy against hepatic carcinoma potentially through immunoregulation. Drug Deliv. **29,** 1983-1993
https://doi.org/10.1080/10717544.2022.2092238

Received: July 10, 2024
Final version accepted: November 10, 2024